PNAS INAUGURAL ARTICLE | IMMUNOLOGY AND INFLAMMATION OPEN ACCESS

Synovial MS4A4A correlates with inflammation and counteracts response to corticosteroids in arthritis

Marie-Astrid Boutet[a,b,1], Irene Mattiola[c,d,1], Rita Silva-Gomes[e,f,g,1], Alessandra Nerviani[a], Marina Sironi[e], Giulia Maria Ghirardi[a], Alessia Troilo[e,h], Stefano Gianoli[e,h,i], Felice Rivellese[a], Cankut Cubuk[a], Katriona Goldmann[a], Anna Rita Putignano[e], Dario Di Silvestre[j], Andrea Lomagno[j], Elena Monica Borroni[e,h], Cristina Sobacchi[e,k], Myles J. Lewis[a], Barbara Bottazzi[e], Massimo Locati[e,h,2], Alberto Mantovani[a,e,l,2,3], and Costantino Pitzalis[a,e,2]

Affiliations are included on p. 10.

This contribution is part of the special series of Inaugural Articles by members of the National Academy of Sciences elected in 2024.
Contributed by Alberto Mantovani; received March 7, 2025; accepted July 31, 2025; reviewed by Lionel B. Ivashkiv and Peter Murray

MS4A4A belongs to the MS4A tetraspan protein superfamily and is selectively expressed by the monocyte–macrophage lineage. In this study, we aimed to evaluate the role of MS4A4A+ macrophages in rheumatoid arthritis (RA) pathogenesis and response to treatment. RNA sequencing and immunohistochemistry of synovial samples from either early treatment-naïve or active chronic RA patients showed that MS4A4A expression positively correlated with synovial inflammation. Synovial macrophages from patients treated with corticosteroids (CS) exhibited an enhanced expression of MS4A4A and Fc γ receptor (FcγR) 3. Accordingly, CS enhanced in vitro the expression of MS4A4A and FcγR3 in human and murine macrophages. In an experimental model of arthritis, Ms4a4a deletion had no effect on the disease course but was associated with enhanced therapeutic response selectively to CS. These results suggest that macrophage expression of MS4A4A represents a biomarker of joint inflammation in RA and that its upregulation in concert with FcγR3 by CS counteracts the therapeutic activity of these drugs. Macrophage MS4A4A may represent a biomarker of joint inflammation in RA and a target to amplify the therapeutic activity of CS.

rheumatoid arthritis | MS4A4A | synovium | macrophages | corticosteroids

Significance

Rheumatoid arthritis (RA) is a chronic joint disease affecting approximately 1% of the population, and about 30 to 40% of RA patients remain unresponsive to available treatments. Macrophages are central cells involved in the pathophysiology of RA. We previously discovered that MS4A4A is a protein selectively expressed by macrophages. In this study, we evaluated the specific role of MS4A4A+ macrophages in RA pathogenesis and response to treatment. These results suggest that macrophage-expressed MS4A4A may represent a biomarker of joint inflammation in RA and a target to amplify the therapeutic activity of corticosteroids.

Rheumatoid arthritis (RA) is the most common chronic inflammatory autoimmune disease affecting joints and causing progressive damage and disability (1). RA is characterized by hyperplasia and inflammatory infiltration of the synovial membrane that leads to cartilage destruction and bone erosion. A wide range of therapeutic options is available to treat RA, including conventional synthetic disease-modifying antirheumatic drugs (csDMARDs) (e.g. methotrexate—MTX) and biologic targeted agents (bDMARDs) working through various mechanisms of actions, including specific inhibition of proinflammatory cytokines (e.g. TNF, IL-6) and signaling pathways (e.g. CTLA4, JAKs) and depletion of infiltrating immune cells (e.g. $CD20^+$ B cells). Despite this extended repertoire of innovative therapeutic options, still today to control active RA symptoms a significant fraction of patients requires administration of corticosteroids (CS), commonly used in conjunction with csDMARDs or as a bridge therapy when starting or switching csDMARDs or bDMARDs. However, the frequent occurrence of adverse events, such as osteoporosis, infections, cardiovascular complications, and treatment resistance, significantly limits the use of CS in inflammatory diseases (2, 3).

Although the mechanisms responsible for disease and treatment response heterogeneity are not entirely clear, the use of next-generation sequencing (NGS) approaches has had a substantial impact on the study of the mechanisms underlying RA pathology (4). Different RA patients exhibit considerable synovial tissue heterogeneity displaying three main prevalent pathotypes: lympho-myeloid, diffuse-myeloid, and pauci-immune, that we and others have shown to associate with disease severity and prognosis as well as therapeutic response (5–13). However, these findings still await to be translated into biomarkers of clinical utility in rheumatology practice and, thus, inadequate response to the available treatments remains a major unmet medical need in RA. Further research is needed to better understand the RA pathogenesis and identify novel therapeutic targets and better predictors of disease prognosis and treatment response.

Nonetheless, the development of therapeutic antibodies targeting TNF and MS4A1/CD20, a member of the membrane-spanning four-domains subfamily A (MS4A) family, represents a major breakthrough in RA therapy (14). The recent development of high-throughput

Reviewers: L.B.I., Hospital for Special Surgery; and P.M., Max Planck Institute for Biochemistry.

Competing interest statement: Co-author C.P. and reviewer L.B.I were co-authors on a 2024 review. The authors declare no other competing interests.

[1]M-A.B., I.M., and R.S.-G. contributed equally to this work.

[2]M.L., A.M., and C.P. contributed equally to this work.

[3]To whom correspondence may be addressed. Email: Alberto.Mantovani@humanitasresearch.it.

This article contains supporting information online at https://www.pnas.org/lookup/suppl/doi:10.1073/pnas.2504529122/-/DCSupplemental.

Published September 9, 2025.

technologies has brought unprecedented insights into synovial inflammation at the single-cell level (15, 16) and held the potential to identify new targets for the development of innovative strategies in RA. Macrophages, highly plastic environment-sensing cells (17–19) have emerged as critical players in the disease pathogenesis and have been shown to be the best synovial biomarker of treatment response (9, 20). The MS4A family, beyond the B cell–specific MS4A1/CD20, comprises 17 other members in humans (21), 5 of which (namely MS4A3, MS4A4A, MS4A6A, MS4A7, and MS4A14) are preferentially expressed in myeloid cells (22, 23). We have reported that CD163$^+$ macrophages in the synovial tissue of early-diagnosed RA patients express high levels of MS4A4A, suggesting an important role in RA pathogenesis (24) similarly to other conditions in which MS4A4A has been shown to regulate macrophage activation including cancer and neurodegenerative disorders. MS4A4A establishes latero-lateral interactions with immune receptors, namely Dectin-1 and TREM-2 (23–26). Notably, MS4A4A expression is enhanced in monocytes and macrophages in response to CS (22, 24).

As the functional role of MS4A4A in RA and its potential association with disease and treatment outcomes is currently unknown, here we evaluated the relationship between MS4A4A expression in human inflamed synovium and clinical outcomes in treatment-naïve patients at early disease stage and in inadequate responders to csDMARDs receiving or not CS before commencing TNF inhibitors treatment, and the role of *Ms4a4a* in a preclinical model of RA in mice with global and macrophage-specific deletion of *Ms4a4a*. We report evidence that MS4A4A expression in macrophages positively correlated with synovial inflammation in synovial samples in early treatment-naïve or active chronic RA patients and that CS selectively induced the expression of MS4A4A and FcγR3 limiting their anti-inflammatory activity and potentially mediating steroid resistance, by enhancing macrophage inflammatory activity.

Results

MS4A4A Expression Correlates with Joint Inflammation and RA Progression. Our previous work showed a specific expression of MS4A4A in CD163$^+$ synovial macrophages of RA patients (24). To define its role in RA pathobiology, we first consulted publicly available transcription datasets and observed that *MS4A4A* was the only member of the MS4A family, among those expressed by the myeloid lineage (22, 23), whose expression was selectively induced in the synovial tissue of RA patients (*SI Appendix*, Fig. S1*A*). The induction of *MS4A4A* was specific for RA and not observed in osteoarthritis or other types of chronic inflammatory arthritis and showed a pattern of expression similar to the B cell–specific *MS4A1/CD20*, which has a well-established role in RA pathogenesis (*SI Appendix*, Fig. S1*A*). Analyses of publicly available scRNAseq datasets revealed that MS4A4A is specifically expressed by TREM2^{high}, FOLR2$^+$ID2$^+$ and FOLR2^{high}LYVE1$^+$ resident macrophages (20) (*SI Appendix*, Fig. S1*B*), all of which also express CD163$^+$. These findings are consistent with our previous work (24). In order to assess the expression of MS4A4A at disease onset in the absence of the influence of immune-suppressive medications, we investigated MS4A4A expression in the synovial tissue of early (< 12 mo symptom duration) DMARD-naïve RA patients (described in *SI Appendix*, Table S1.). Both at the transcript and protein level, MS4A4A expression was associated with the diffuse-myeloid and lympho-myeloid pathotypes (Fig. 1 *A*–*D*), the latest being characterized by a high infiltration of macrophages and lymphocytes organized in ectopic lymphoid structures, known to sustain autoantibodies production and associated with high disease activity and radiographic damages (5, 6, 8, 27). MS4A4A expression positively correlated with the synovial infiltration of lining and sublining CD68$^+$ macrophages, CD3$^+$ T cells, CD20$^+$ B cells, and CD138$^+$ plasma cells, as well as with the global synovial inflammatory score (Fig. 1 *E* and *F*). We also found a significant positive correlation between synovial MS4A4A gene and protein expression and clinical parameters indicative of disease severity, including the disease activity score DAS28 (Fig. 1*G*) and the erythrocyte sedimentation rate (ESR) (Fig. 1*H*). Both the diffuse-myeloid and the lympho-myeloid pathotypes were characterized by an important infiltration of CD68$^+$ macrophages (*SI Appendix*, Fig. S2*A*), but the absence of direct correlation between the total CD68 score and the DAS28 suggested a specific contribution of a MS4A4A$^+$ macrophage subset to the activity of the disease (*SI Appendix*, Fig. S2*B*).

Of note, RNA-seq analysis of synovial tissue from RA patients also revealed a positive correlation between expression levels of *MS4A4A* and proinflammatory mediators (*IL1B* and *TNF*), neutrophil chemoattractants (*CXCL1* and *CXCL8)*, and genes promoting bone resorption (*MMP1/3* and *13, RANK, RANKL*) and a negative correlation with gene preventing bone resorption (*OPG*, coding for the decoy receptor of RANKL) (Fig. 1*I*). Accordingly, a positive correlation between the frequency of MS4A4A$^+$ cells and neutrophils was also observed in the synovial tissue of patients with both early and established disease (Fig. 1*J*). A high expression of MS4A4A in the synovium at the onset of RA was associated with a high degree of bone erosions assessed by the total SHSS, both at baseline and at 12 mo following patients' recruitment (Fig. 1*K*).

To better understand the relationship between MS4A4A expression on macrophages and RA pathogenesis, we adopted the experimental model of STIA. Increased *Ms4a4a* expression was observed at the peak of inflammation (Day 6 upon STIA induction) compared to the early stage of inflammation (Day 2) and persisted over time (until Day 12) compared to the early stage of inflammation (Day 2), along with enhanced joint inflammation and clinical scores (Fig. 1 *L* and *M*). Of note, *Ms4a4a* expression positively correlated with the arthritis score (Fig. 1*N*), and no difference was observed in the frequency of synovial CD11b$^+$ F4/80$^+$ MHCII$^-$ macrophages (Fig. 1*O*). This indicates that the increased expression of *Ms4a4a* was not just a secondary effect of the general increase in macrophage infiltrate, but rather of a specific modulation in the MS4A4A$^+$ cell subset. However, mice with either constitutive deletion (from now on *Ms4a4a*-KO) or a macrophage-selective conditional deletion of the *Ms4a4a* gene (*Ms4a4d$^{fl/fl}$ x Lyz2$^{Cre/+}$*, from now on *Ms4a4a*-cKO) did not show differences in STIA severity compared to their littermate controls (Fig. 1*L* and *SI Appendix*, Fig. S2*C*), indicating that MS4A4A has no direct impact on the effector phase of the disease.

MS4A4A Expression in Macrophages Is Modulated by CS Therapeutic Treatment. We then investigated the potential role of MS4A4A in established RA, when the pathology becomes chronic, and patients undergo therapeutic treatment. We first compared MS4A4A expression in the synovial tissue obtained from the early treatment-naïve patients described above and from patients with established RA (mean disease duration of 4.6 vs. 61.1 mo in the two cohorts, respectively). As reported in *SI Appendix*, Table S2., these patients are characterized by a high number of tender joints and high scores for Visual Analogue Scale (VAS) physician and DAS28, indicative of their persistent active disease despite therapeutic treatments. Compared to early-diagnosed patients, chronic RA patients showed a higher frequency of MS4A4A$^+$ cells in their synovial tissue (Fig. 2*A*). In this cohort,

MS4A4A expression also associated with the lympho-myeloid and the diffuse-myeloid pathotypes, and with a prominent joint inflammation and synovial immune cell infiltration (Fig. 2 *B* and *C*). Opposite to the patients included in the early treatment-naïve RA cohort, all patients included in the established RA cohort underwent csDMARD treatments (*SI Appendix*, Table S2.), and 35.7% of them also received CS. To investigate the effect of different therapeutic regimens on MS4A4A expression, the synovial tissue of patients treated with csDMARDs alone was compared to that of patients treated with both csDMARDs and CS. CS treatment did not affect the overall macrophage infiltration in the synovium (Fig. 2 *D* and *E*) but significantly enhanced MS4A4A expression levels (Fig. 2 *F* and *G*), suggesting a direct effect of CS on the modulation of MS4A4A expression in synovial macrophages. Consistent with previous data (20, 24), MS4A4A expression was distributed across both lining and sublining synovial layers. We showed a significant CS-dependent upregulation of MS4A4A in the sublining macrophages and a trend of induction in the lining (Fig. 2*H*). Since induced expression of MS4A4A in the RA patients was in line with our previous evidence that CS directly regulate *Ms4a4a* in murine bone marrow–derived macrophages (BMDM) (24), we investigated *Ms4a4a* expression in synovial macrophages isolated from murine arthritic joints treated with or without CS. We observed that synovial macrophages (sMac) expressed significantly higher *Ms4a4a* basal levels compared to both BMDM and peritoneal macrophages (pMac) and that also in murine synovial macrophages *Ms4a4a* expression was further induced upon in vitro treatment with CS, namely dexamethasone (Dex) (Fig. 2*I*). Of note, *Ms4a4a* was not expressed at baseline neither was induced after Dex treatment in fibroblast-like synoviocytes, a second key player in the formation of the synovial pannus in the STIA model (Fig. 2*I*). In addition, the induction of *Ms4a4a* expression in peritoneal macrophages was also observed after in vivo administration of CS (Fig. 2*J*).

MS4A4A Expression in Macrophages Limits CS Therapeutic Activity in Arthritis. We then investigated the relevance of MS4A4A for joint inflammation and RA progression upon CS treatment. The therapeutic activity of Dex was significantly enhanced in *Ms4a4a*-KO mice (Fig. 3*A*) and in *Ms4a4a*-cKO mice (*SI Appendix*, Fig. S2*C*), as demonstrated by the lower arthritis scores particularly in the KO animals, suggesting that treatment activity was indeed influenced by Ms4a4a expression in macrophages. Of note, *Ms4a4a* deletion did not influence the efficacy of other in vivo therapeutic regimens with different mechanism of action, including MTX (Fig. 3*B*) and intravenous immunoglobulins (IVIg) (Fig. 3*C*). In keeping with this, MTX and IVIg also did not modulate *Ms4a4a* expression by macrophages in vitro (Fig. 3*D*), contrary to effects seen with CS treatment. In accordance with the clinical scores, the synovial pannus of *Ms4a4a*-KO mice treated with Dex showed a significant reduction in the number of inflammatory cells compared to Dex-treated WT mice (Fig. 3 *E* and *F*). Taken together, these results suggest a potential feedback loop between MS4A4A and CS, with CS inducing MS4A4A expression in macrophages, which in turn limits their therapeutic activity in arthritis.

MS4A4A Expression Is Associated with Synovial Neutrophil Infiltration and Joint Damage Upon CS Treatment. The ability of Ms4a4a to interfere with CS treatment and promote joint inflammation in arthritis prompted us to investigate its impact on the recruitment of inflammatory immune cells to the joint. Dex treatment did not influence the number of macrophages or monocytes infiltrating the joint (*SI Appendix*, Fig. S3 *A*–*D*). Conversely, we observed a reduced infiltration of $Ly6G^+$ neutrophils, which have a crucial role in the progression and the perpetuation of joint inflammation in the STIA model (30), in *Ms4a4a*-KO joints compared to controls upon Dex treatment (Fig. 4 *A*–*D*). This correlated with neutrophil accumulation in the blood and was not due to an altered neutrophil granulopoiesis in the bone marrow (*SI Appendix*, Fig. S3 *E* and *F*).

Arthritic joints of *Ms4a4a*-KO mice treated with Dex also showed reduced damage of cartilage and bone tissue, defined by reduced number of $TRAP^+$ resorbing osteoclasts (Fig. 4 *E* and *F*) as well as a delayed upregulation of Dex-dependent genes involved in bone resorption (*Rankl*/*Opg* ratio) (Fig. 4*G*) and cartilage matrix degradation (matrix metalloproteinase *Mmp3*) (Fig. 4*H*). Taken together, these results indicated that MS4A4A contributes to the modulation of neutrophil recruitment and bone and cartilage erosion in synovial inflammation upon CS treatment.

Expression of MS4A4A and FCGR3A Is Concomitantly Enhanced by CS. MS4A4A is a tetraspan-like molecule that, similar to classical tetraspanins (31), is involved in the modulation of certain immune receptor intracellular pathways contributing to macrophage activation and thus sustaining inflammatory immune responses (23). In particular, we previously demonstrated that MS4A4A associates with Dectin-1 (24), and others have reported its association with TREM-2 (25). We therefore searched for evidence that macrophage immune receptors known to be modulated by MS4A4A could be involved in this phenotype. In early treatment-naïve RA patients, at the gene level (RNA-seq) we observed a positive correlation between the expression of *MS4A4A* and both molecules (*SI Appendix*, Fig. S4*A*), while multiplex immunofluorescence (IF) staining of RA synovial macrophages showed coexpression of MS4A4A and Dectin-1, as well as of MS4A4A and TREM-2 (*SI Appendix*, Fig. S4*B*). However, in contrast to what observed for MS4A4A (Fig. 1 *G* and *H*), the expression of Dectin-1 and TREM-2 correlated with synovial histopathology but not with disease severity (*SI Appendix*, Fig. S4 *C*–*F*). Furthermore, in mice, the Dex-dependent induction (Figs. 2*H* and 3*D*) was not observed neither for *Clec7a* (encoding Dectin-1) nor for *Trem2* (*SI Appendix*, Fig. S4*G*). These data argue against a role of the known MS4A4A partners Dectin-1 and TREM-2 in mediating the MS4A4A-dependent limitation of the CS anti-inflammatory activity in joint inflammation and arthritis progression under CS treatment.

Fc receptors, and particularly FcγR3-mediated responses, have a pivotal role in the pathogenesis of RA and in the STIA model (30, 32, 33). RNA-sequencing analyses of the synovium of early treatment-naïve RA patients showed that the expression of both *FCGR3A* and its signal transducer Fc common gamma chain (*FCER1G*) positively correlated with *MS4A4A* expression (Fig. 5*A*), with related protein coexpression shown by multiplex IF staining (Fig. 5*B*). *FCGR3A* expression was high in both the diffuse-myeloid and lympho-myeloid pathotypes and significantly correlated with the disease severity (Fig. 5 *C* and *D*), in line with *MS4A4A* (Fig. 1 *A*–*H*) but opposite to *CLEC7A* and *TREM2* (*SI Appendix*, Fig. S4 *C*–*F*). We next investigated the effect of CS and showed that in accordance with *Ms4a4a* (Figs. 2*H* and 3*D*) but conversely to *Clec7a* and *Trem2* (*SI Appendix*, Fig. S4*G*), Dex treatment induced the expression of *Fcgr3a* both in WT and *Ms4a4a*-KO macrophages (Fig. 5*E*), while no effect on other Fc receptors was observed (*SI Appendix*, Fig. S4*H*). It should be noted that transcriptional profiling of WT and *Ms4a4a*-deficient macrophages revealed no difference at baseline and in response to CS (*SI Appendix*, Fig. S5). As reported for MS4A4A (Fig. 2 *F* and *G*), FCGR3A was induced upon CS treatment in our cohort of

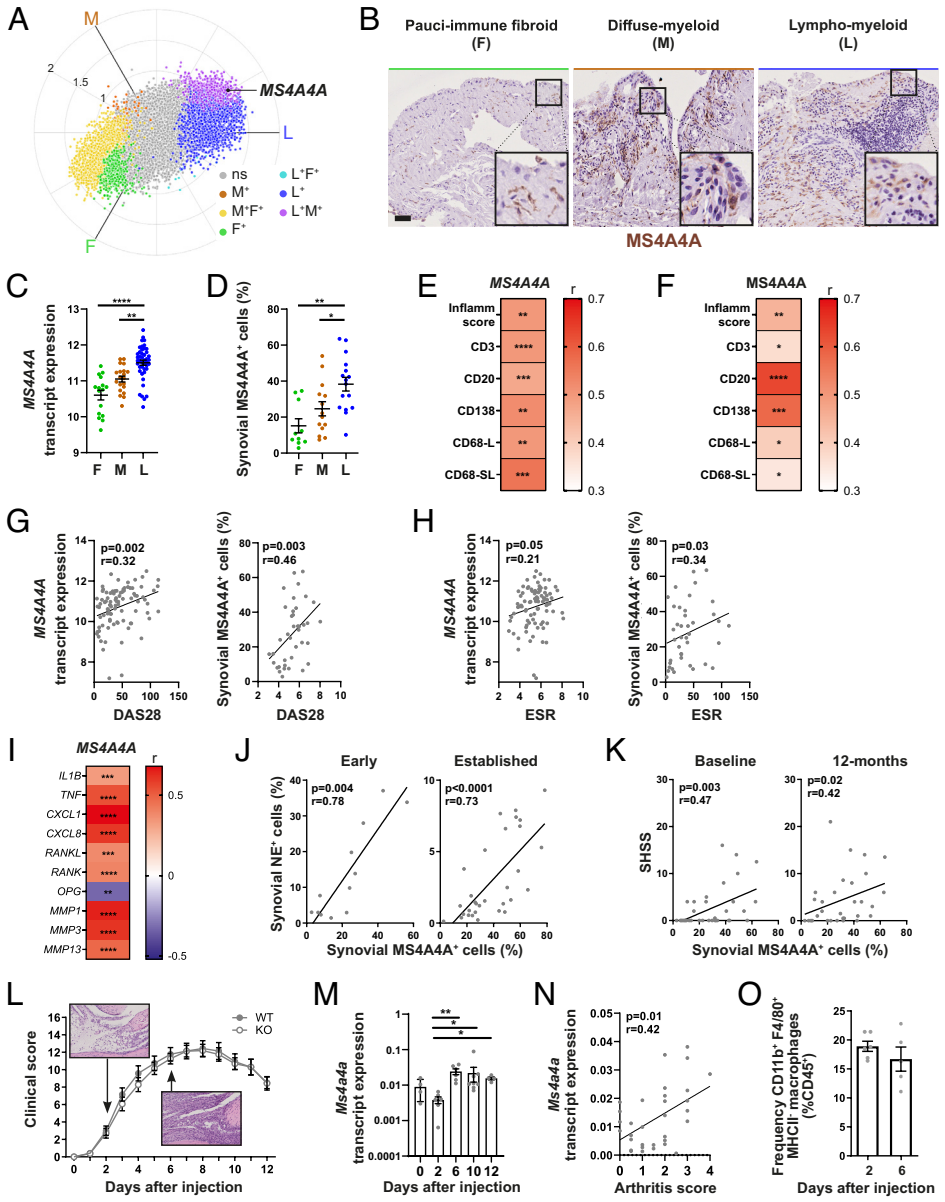

Fig. 1. MS4A4A expression correlates with joint inflammation and RA progression. (*A*) 2D polar plot of differentially expressed genes, assessed by RNA-sequencing, comparing synovial tissue presenting a lympho-myeloid (L), diffuse-myeloid (M), and pauci-immune fibroid (F) pathotypes (6). The z-axis shows–log10 *P*-value for likelihood ratio test. Genes with adjusted *P*-value for likelihood ratio test < 0.05 (z axis) were considered significant (nonsignificant genes are colored gray). Different colors demonstrate pairwise comparisons between the three pathotypes: upregulation in one group only (M: brown, F: green, and L: blue) or in two groups (M + F: yellow, L + F: cyan, L + M: purple). (*B*) Sections of RA synovium were stained for MS4A4A. Representative images are shown for each pathotype. Enlarged images correspond to the respective boxed areas. (Scale bar, 50 μm.) (*C*) *MS4A4A* transcript expression in synovial tissues presenting an F, M, or L pathotype, assessed by RNA-sequencing. *P*-values were calculated using the Kruskal–Wallis test with Dunn's posttest, $^{**}P < 0.01$, $^{****}P < 0.0001$. (*D*) Percentage of MS4A4A$^+$cells in synovial tissues presenting an F, M, or L pathotype, assessed by immunohistochemistry (IHC) and quantified by digital image analysis. *P*-values were calculated using the Kruskal–Wallis test with Dunn's posttest, $^{*}P < 0.05$, $^{**}P < 0.01$. (*E*) Heatmap representing the correlation between *MS4A4A* synovial transcript levels and the semiquantitative scores for synovitis (Inflamm. Score) and inflammatory cell markers (CD3$^+$ T cells; CD20$^+$ B cells; CD138$^+$ plasma cells; CD68L$^+$ macrophages of the lining layer; CD68SL$^+$ macrophages of the sublining layer) (28, 29). The red scale represents the Spearman r coefficient. $^{**}P < 0.01$, $^{***}P < 0.001$, $^{****}P < 0.0001$. (*F*) Heatmap representing the correlation between MS4A4A expression and the semiquantitative scores for inflammatory cell markers (CD3$^+$ T cells; CD20$^+$ B cells; CD138$^+$ plasma cells; CD68L$^+$ macrophages of the lining layer; CD68SL$^+$ macrophages of the sublining layer) in early-treatment naïve patients. The red scale represents the Spearman r coefficient. $^{*}P < 0.05$, $^{**}P < 0.01$, $^{***}P < 0.001$, $^{****}P < 0.0001$. (*G* and *H*) Correlation of *MS4A4A* transcript (*Left* panels) and protein (*Right* panels) expression with the disease activity score/28 (DAS28) (*G*) and the ESR (*H*). *P*-value and r coefficient were calculated using the Pearson correlation test. (*I*) Heatmap representing the correlation between *MS4A4A* synovial transcript levels in patients with early untreated RA and different mediators involved in tissue inflammation and neutrophil recruitment (*IL1B*, *TNF*, *CXCL1*, and *CXCL8*), and in bone and cartilage destruction (*RANKL*, *RANK*, *OPG*, and *MMP1*, *3*, and *13*). The blue/red scale represents the Spearman r coefficient. $^{**}P < 0.01$, $^{***}P < 0.001$, $^{****}P < 0.0001$. (*J*) Correlation between the percentage of MS4A4A$^+$ cells and the percentage of neutrophil-elastase$^+$ (NE) cells in the synovial tissue of early naïve RA (*Left* panel) or established RA patients (*Right* panel). *P*-values and r coefficients were calculated according to the Pearson correlation test. (*K*) Correlation between the percentage of MS4A4A$^+$ cells and the presence of erosions at baseline (*Left* panel) and at 12 mo (*Right* panel) as assessed by the total Sharp van der Heijde score (SHSS) in early treatment naïve RA patients. *P*-values and r coefficients were calculated according to the Pearson correlation test. (*L*) Clinical score assessing forepaws and hind paws inflammation (/16) after serum transfer-induced arthritis (STIA) induction in wild-type (WT) (gray dots) and Ms4a4a knock-out (KO) (empty gray dots) mice. N = 20 to 22 animals per group. Representative hematoxylin & eosin (H&E) staining of the synovium at day 2 and day 6 is shown. (*M*) *Ms4a4a* relative gene expression assessed by qPCR on total joints of naïve and STIA WT mice at day 2, day 6, day 10, and day 12 following arthritis induction. *P*-values were calculated using the Kruskal–Wallis test with Dunn's posttest, $^{**}P < 0.01$. (*N*) Correlation between *Ms4a4a* relative expression and arthritis score (/4) for each individual paw (n = 33, distributed across day 2, day 6, and day 12 timepoints). *P*-value and r coefficient were calculated according to the Spearman correlation test. (*O*) Frequency of CD11b$^+$ F4/80$^+$ MHCII$^-$ macrophages, expressed in % of total live CD45$^+$ cells, in the joints at day 2 and day 6 after STIA induction. (*C*, *D*, *L*, *M*, and *O*) Results are shown as mean ± SEM.

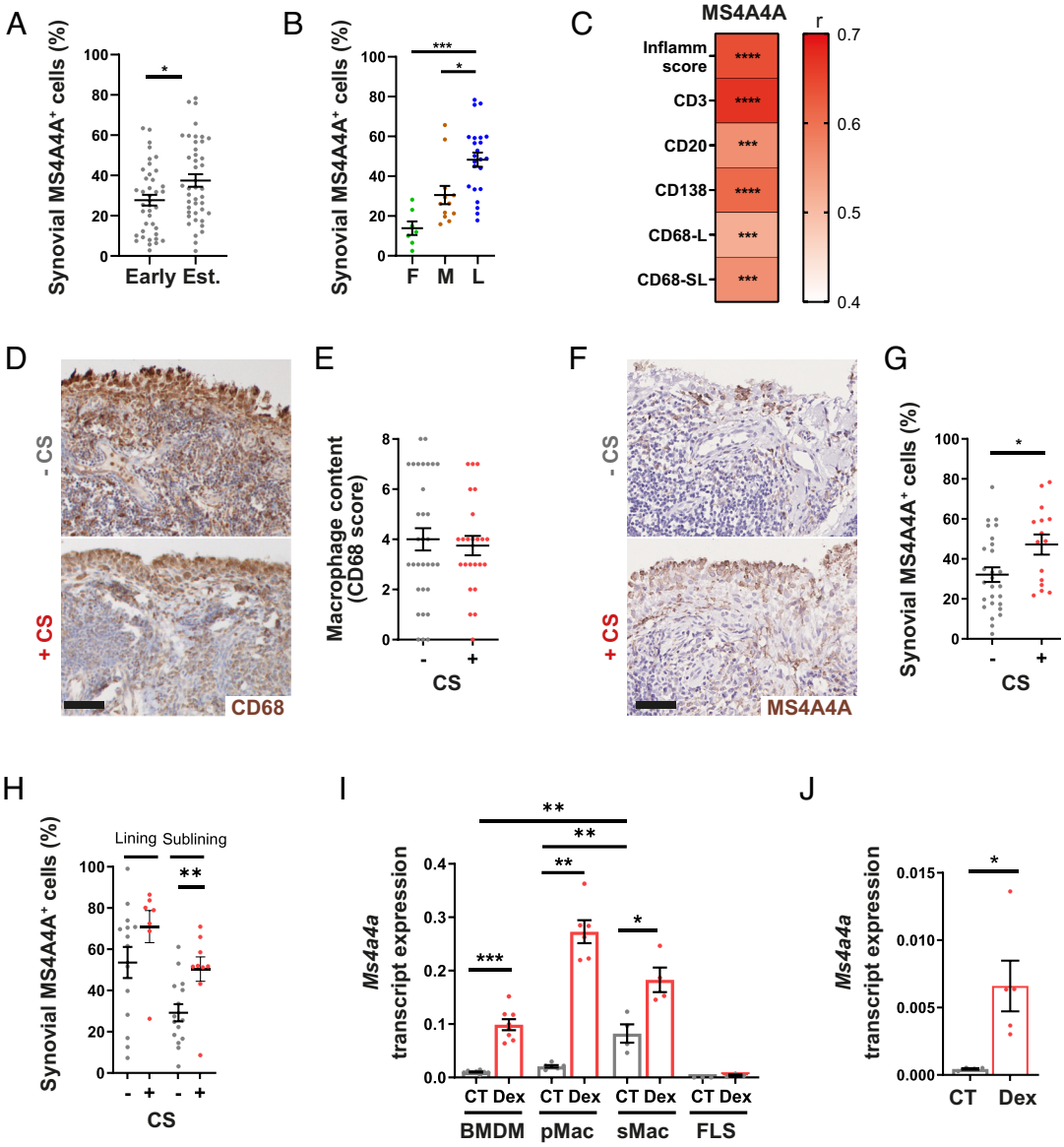

Fig. 2. MS4A4A expression in macrophages is upregulated by CS treatment. (*A*) Percentage of MS4A4A$^+$ cells in the synovial tissues of patients with early and established (est.) RA, assessed by IHC and quantified by digital image analysis. *P*-values were calculated using the Student *t* test. *$P < 0.05$. (*B*) Percentage of MS4A4A$^+$ cells in synovial tissues of established RA patients presenting a pauci-immune fibroid (F), diffuse-myeloid (M), or lympho-myeloid (L) pathotype. *P*-values were calculated using the Kruskal–Wallis test with Dunn's posttest, *$P < 0.05$, ***$P < 0.001$. (*C*) Heatmap representing the correlation between MS4A4A expression and the semiquantitative scores for inflammatory cell markers (CD3$^+$ T cells; CD20$^+$ B cells; CD138$^+$ plasma cells; CD68L$^+$ macrophages of the lining layer; CD68SL$^+$ macrophages of the sublining layer) in established patients. The red scale represents the Spearman r coefficient. ***$P < 0.001$, ****$P < 0.0001$. (*D*) Synovial tissues of patients who did or did not receive corticosteroid (CS) treatment in adjunction with conventional synthetic disease-modifying antirheumatic drugs were stained for CD68 by IHC. Representative images are shown. (Scale bar, 50 µm.) (*E*) CD68 lining and sublining macrophages semiquantitative score (CD68 score) in the synovium of RA patients treated or not with CS. (*F*) Synovial tissues of patients who did or did not receive CS treatment were stained for MS4A4A by IHC. Representative images are shown. (Scale bar, 50 µm.) (*G* and *H*) Percentage of MS4A4A$^+$ cells quantified by digital image analysis in the synovium of RA patients treated or not with CS, in the whole synovial tissue (*G*) and separately in the lining and sublining areas (*H*). *P*-values were calculated using the Mann–Whitney test, *$P < 0.05$, **$P < 0.01$. (*I*) *Ms4a4a* transcript expression in BMDM, peritoneal macrophages (pMac), primary synovial macrophages (sMac), and primary fibroblast-like synoviocytes (FLS) isolated from arthritic joints of WT animals and kept untreated (control, CT) or treated with 1 µM dexamethasone (Dex) for 6 h (Dex). N = 3 to 8 per group. *P*-values were calculated using the Mann–Whitney test, *$P < 0.05$, **$P < 0.01$, ***$P < 0.001$. (*J*) *Ms4a4a* transcript expression in peritoneal exudate cells (PEC) of WT mice 2 h following intraperitoneal injection of PBS (CT) or 10 µg Dex. *P*-values were calculated using the Mann–Whitney test. *$P < 0.05$. n = 4-5 mice per group. (*A*, *B*, *E*, *G*, *H*, *I*, and *J*) Results are shown as mean ± SEM.

established RA patients (Fig. 5 *F* and *G*) and a significant positive correlation between the expression of MS4A4A and the expression of FCGR3A was observed (Fig. 5*H*).

We then evaluated whether MS4A4A could regulate the activity of FCGR3 and sustain joint inflammation, particularly neutrophil recruitment and activation. When triggered with aggregated IgG complexes, macrophages derived from *Ms4a4a*-KO animals showed a reduced ability to secrete Tnf and Cxcl2, proinflammatory mediators with a key role in joint inflammation and neutrophil recruitment in RA pathogenesis (34), and this defect was further enhanced after Dex treatment in vitro (Fig. 5*I*). Of note, Ms4a4a did not significantly affect macrophage LPS-dependent responses, neither under resting conditions nor upon CS treatment, arguing for a specific effect of Ms4a4a on macrophage activation by FcγR-dependent pathways (Fig. 5*I*). Importantly, the same reduction in Tnf and *Cxcl2* upon CS treatment was observed in arthritic joints in the STIA model (Fig. 5*J*). Together, these data suggest that MS4A4A and FcγR3 are coregulated in RA with MS4A4A

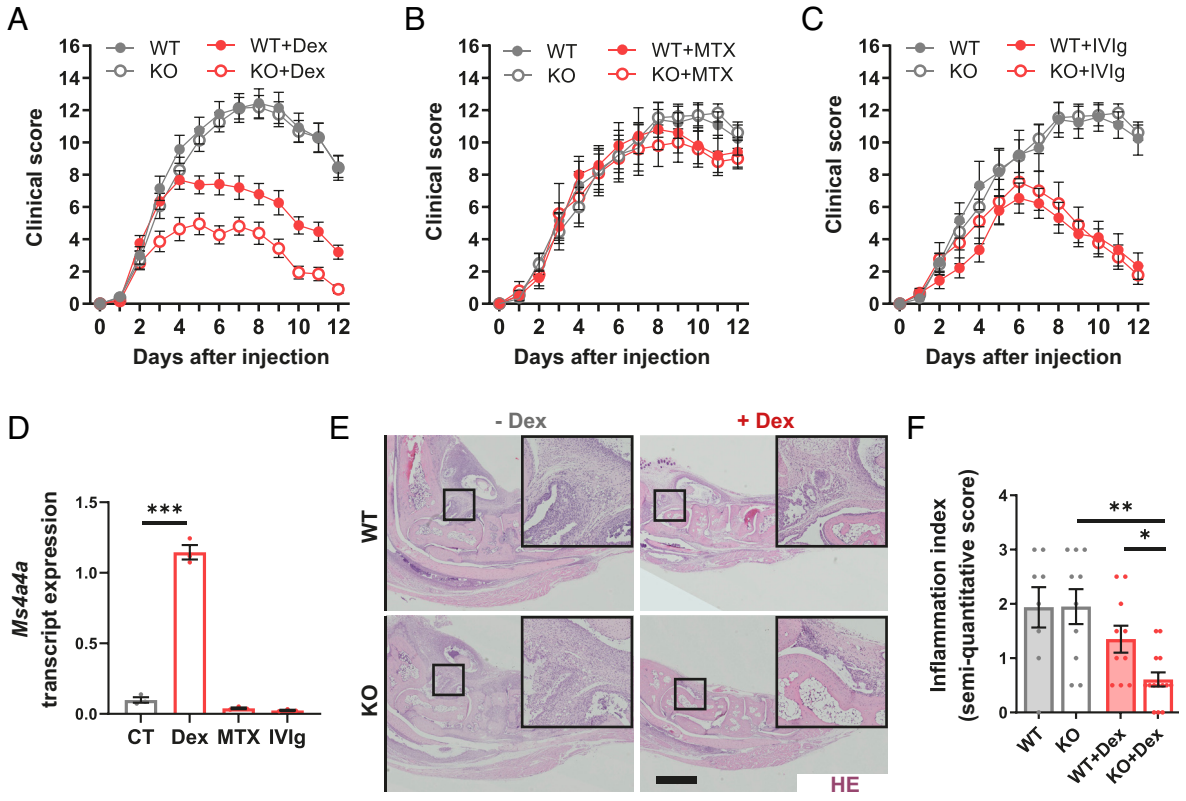

Fig. 3. MS4A4A expression in macrophages limits the CS therapeutic activity in arthritis. (*A*) Clinical score assessing forepaws and hind paws inflammation after STIA induction in wild-type (WT) (plain dots) and *Ms4a4a* knock-out (KO) (empty dots) mice, injected intraperitoneally daily from D2 with 10 μg dexamethasone (Dex, red lines) or its vehicle (100 μL PBS) (gray lines). N = 20 to 22 animals per group. Scores of the KO+Dex group are significantly lower compared WT+Dex from day 3 ($P < 0.01$, as assessed by the two-way ANOVA test followed by Tukey's multiple comparisons). (*B*) Clinical score after STIA induction in WT (plain dots) and *Ms4a4a*-KO (empty dots) mice, injected intraperitoneally 25 μg methotrexate (red lines) or with PBS (gray lines) every 2 d from D2. N = 5 to 12 animals per group. Scores of the WT+MTX and KO+MTX groups do not statistically differ from untreated corresponding animals (as assessed by the two-way ANOVA test followed by Tukey's multiple comparisons). (*C*) Clinical score after STIA induction in WT (plain dots) and *Ms4a4a*-KO (empty dots) mice treated with a single intraperitoneal injection at day 2 of 2 mg/kg intravenous immunoglobulin (IVIg, red lines) or with PBS (gray lines). N = 5 to 12 animals per group. WT+IVIg and KO+IVIg scores are similarly and significantly reduced compared to untreated WT and KO from day 8 ($P < 0.05$, as assessed by the two-way ANOVA test followed by Tukey's multiple comparisons). (*D*) *Ms4a4a* transcript expression in BMDM stimulated with IL-4 alone (CT) or in combination with 1 μM of Dex, 5 ng/mL of methotrexate (MTX) or 80 μg of intravenous immunoglobulin (IVIg) for 18 h. n = 3 per group. *P*-values were assessed using the Mann–Whitney test, ***$P < 0.001$. (*E*) Sections of tarsus from WT and KO arthritic mice treated or not with 10 μg Dex were stained with H&E. Representative images are shown for each group. Enlarged images correspond to the respective boxed areas. (Scale bar, 1 mm.) (*F*) Semiquantitative scores (0 to 3) were attributed for each tarsus stained with H&E at day 6 after STIA induction. n = 8 to 12 individual paws per group. *P*-values were calculated using the Kruskal–Wallis test with Dunn's posttest, *$P < 0.05$, **$P < 0.01$. (*A*–*D* and *F*) Results are shown as mean ± SEM.

restraining the anti-inflammatory effect of CS and potentially regulating the inflammatory function of FcγR.

Discussion

MS4A1/CD20, the best characterized member of the tetraspan-like family MS4A, is selectively expressed in B cells, where it modulates the B cell receptor (BCR) signaling (35) and is a validated therapeutic target in autoimmune diseases and cancer (36, 37). Similarly, MS4A4A is selectively expressed in macrophages where it partners and modulates signaling activities of the innate immunity receptors Dectin-1 and TREM-2 (24–26). As macrophages are major players in inflammation and autoimmunity, including RA (16), the present study was designed to investigate the expression and significance of MS4A4A in RA and to explore its function in genetically modified animals.

It has previously been reported that in mice and humans, MS4A4A is highly expressed in mature tissue macrophages, including those in the synovium, and low levels are present in circulating monocytes (23, 24). More recently, it was shown that MS4A4A is expressed at low levels in healthy $CD14^+CD16^+$, $CD14^+CD16^-$, and $CD16^-CD14^+$ monocyte subsets, and is overexpressed in septic conditions in both $CD14^+CD16^+$ and $CD14^+CD16^-$ monocytes (38). It was important to reassess MS4A4A expression in peripheral blood monocytes in RA. Therefore, we retrieved publicly available bulk RNA-sequencing data from $CD14^+$ circulating monocytes isolated from 15 healthy controls and 9 RA patients (GSE294225), observing that *MS4A4A* expression is not affected in RA monocytes compared to controls (*SI Appendix*, Fig. S6).

We previously reported high expression levels of MS4A4A in the $CD163^+$ macrophage subset infiltrating the synovial tissue of RA patients (24). Here, we provide evidence that its expression is associated with high levels of inflammation/disease activity and worse outcomes, both in treatment-naïve early RA, prior to disease modification by immune-modulatory therapy, and in established active disease resistant to csDMARDs treatment. Similar to the B cell–specific MS4A1/CD20, the macrophage-specific MS4A4A is significantly elevated in RA and not in osteoarthritis or other inflammatory arthritis. Accordingly, *MS4A4A* has recently been shown to be part of the gene signature expressed in peripheral leukocytes from RA but not in patients with undifferentiated arthritis or healthy controls (39). *MS4A4A* expression in blood is also related with the occurrence of RA-associated interstitial lung disease, one of the most common extra-articular manifestations of the disease (40). Our results show that MS4A4A is highly

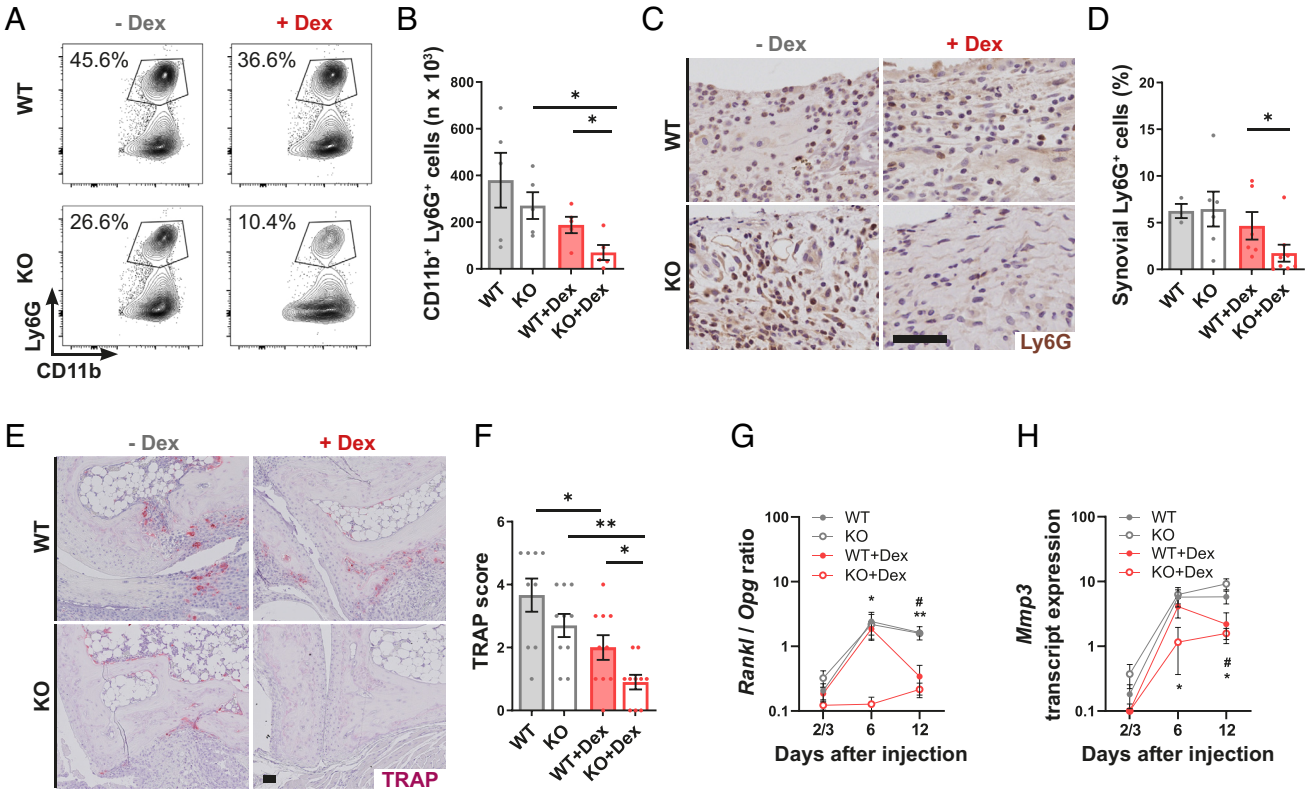

Fig. 4. MS4A4A expression is associated with synovial neutrophil infiltration and joint damage upon CS treatment. (*A*) Representative dot plots of the frequency of Ly6G$^+$ neutrophils gated as CD11b$^+$ Ly6G$^+$ on live CD45$^+$ in the synovium of *Ms4a4a* wild-type (WT) and knock-out (KO) mice treated or not with dexamethasone (Dex) at day 6 following STIA induction. (*B*) Absolute count of Ly6G$^+$ neutrophils determined in the mouse arthritic synovium by flow cytometry at day 6 after STIA induction. N = 5 mice per group. *P*-values were calculated using the Kruskal–Wallis test with Dunn's posttest, *$P < 0.05$. (*C*) Mouse ankle joints collected at day 6 after STIA induction and treated or not with Dex were stained for Ly6G by IHC. Representative images are shown. (Scale bar, 50 μm.) (*D*) Percentage of Ly6G$^+$ cells in the synovium of WT and KO mice treated or not with Dex at day 6 after STIA induction, assessed by IHC and quantified by digital image analysis. N = 3 to 8 individual paws per group. *P*-values were calculated using the Kruskal–Wallis test with Dunn's posttest, *$P < 0.05$. (*E*) Mouse ankle joints collected at day 12 after STIA induction in *Ms4a4a* WT and KO mice treated or not with Dex were stained for tartrate-resistant acid phosphatase (TRAP) to reveal the presence of osteoclasts. Representative images are shown. (Scale bar, 50 μm.) (*F*) Semiquantitative scores (0 to 5) attributed for each tarsus stained with TRAP at day 12 after STIA induction. N = 9 to 10 individual paws per group. *P*-values were calculated using the Kruskal–Wallis test with Dunn's posttest, *$P < 0.05$, **$P < 0.01$. (*G*) Ratio of the relative expression of *Rankl* and *Opg* transcripts in the ankles of WT and KO mice treated or not with 10 μg Dex at different time-points after STIA induction. N = 4 to 7 mice per group and per time-point. * and ** indicate that KO and KO+Dex values are significantly different at both day 6 and day 12 ($P < 0.05$ and $P < 0.01$, respectively), # indicates that WT and WT Dex values are similar at D6 and significantly differ only at day 12 ($P < 0.05$, as assessed by the two-way ANOVA test followed by Tukey's multiple comparisons). (*H*) *Mmp3* gene expression in the ankles of WT and KO mice treated with PBS or Dex at different time-points after STIA induction. N = 4 to 7 mice per group and per time-point. * indicates that KO and KO+Dex values are significantly different at both day 6 and day 12 ($P < 0.05$), # indicates that WT and WT Dex values are similar at day 6 and significantly differ only at day 12 ($P < 0.05$, as assessed by the two-way ANOVA test followed by Tukey's multiple comparisons). (*B*, *D*, and *F*–*H*) Results are shown as mean ± SEM.

expressed in synovial tissues presenting a lympho-myeloid pathotype, which is characterized by a high infiltration of macrophages and/or lymphocytes organized in ectopic lymphoid structures, known to sustain autoantibodies formation and associated with high disease activity and radiographic damages (5, 6, 8, 27). Accordingly, we observed that synovial MS4A4A expression in early treatment-naïve RA patients significantly associated with baseline disease activity and structural damage predicting worse SHSS erosion score at 12 mo. Whether MS4A4A regulates osteoclast-mediated bone erosions in the context of RA will require future investigations, however our synovial tissue RNA-seq analysis demonstrating a positive correlation with gene enhancing bone resorption: RANK/RANKL and a negative correlation with the gene preventing bone resorption: *OPG*, suggests its potential involvement.

Glucocorticoid hormones are part of physiological regulatory pathways of inflammation and immunity (41) and have complex effects on immunity beyond suppression (42). In particular, CS are known to strongly influence monocytes/macrophage biology, shaping their phenotype toward repair functions (43). *MS4A4A* has previously been reported as a CS-responsive gene, both in vitro in monocyte-derived macrophages and in vivo in circulating monocytes of Graves's syndrome patients (24, 44). Here, we report that CS treatment increases MS4A4A expression, both in human RA synovium and in the joint of arthritic mice, a finding consistent with previous in vitro observations on human macrophages (22, 24). Thus, the induction of MS4A4A in macrophages is part of the complex effect elicited by GC on inflammatory networks. Recent evidence suggests that changes in macrophage metabolism and itaconate production play an important role in the anti-inflammatory activity of CS (45). In synovial tissue from early treatment-naïve RA patients (PEAC cohort), we found no correlation between Aconitate Decarboxylase 1 (CAD/ACOD1) and MS4A4A expression (*SI Appendix*, Fig. S7 *A* and *B*). Moreover, analysis of the data reported by Auger et al. revealed that *Ms4a4a* is regulated to a similar extent by CS in wild-type and ACOD1-deficient mice (*SI Appendix*, Fig. S7*C*) (45). These results strongly suggest the *Ms4a4a* induction by CS is independent of ACOD1.

In an effort to explore the functional significance of MS4A4A in RA, a model of serum-transfer induced arthritis in genetically modified mice was used. Ms4a4a deficiency had no impact on the severity of the disease. In contrast, Ms4a4a deficiency was associated with a significant increase in the therapeutic action of CS. Indeed, CS-treated *Ms4a4a*-deficient arthritic mice showed

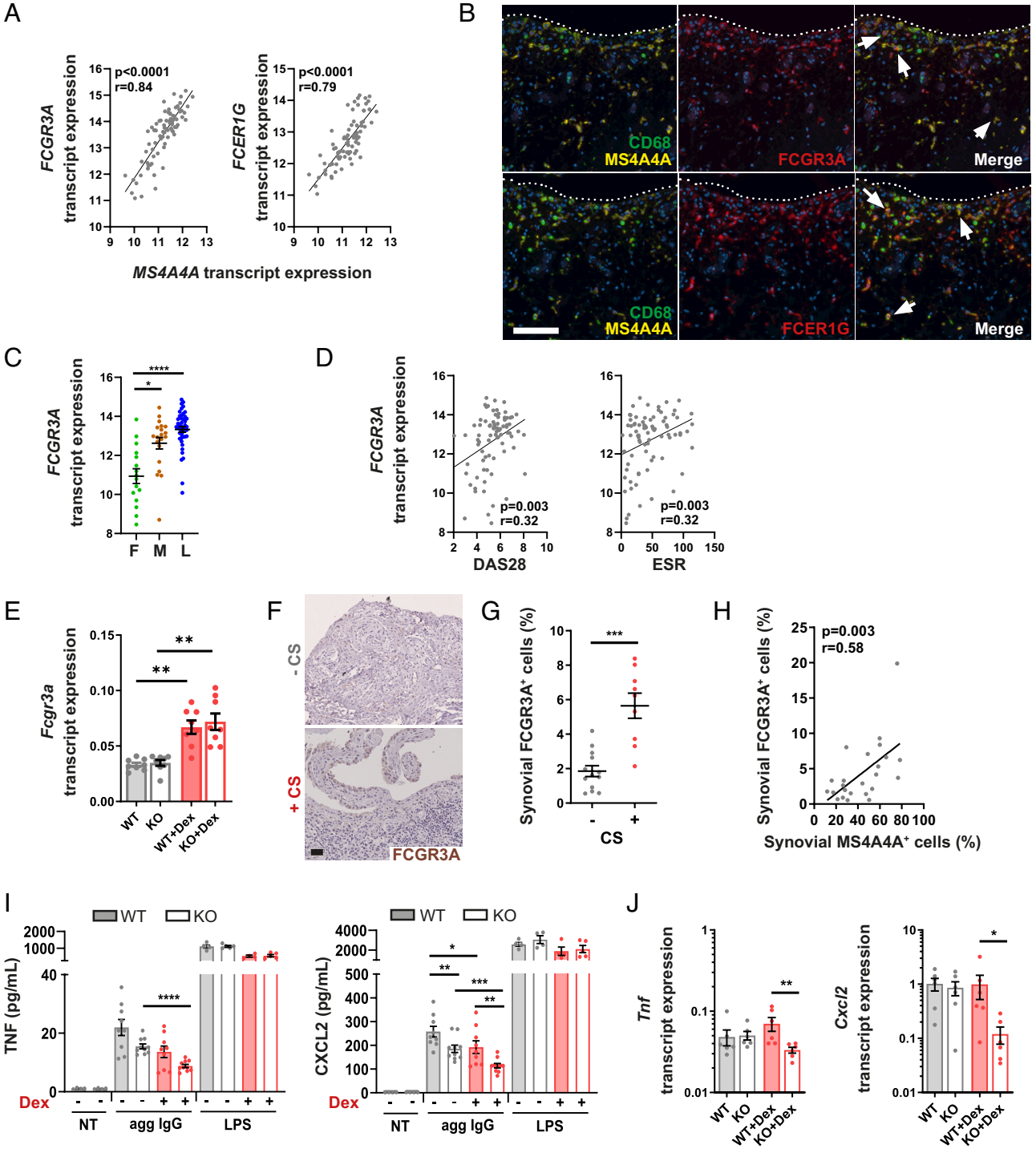

Fig. 5. Expression of MS4A4A and FCGR3A is concomitantly enhanced by CS. (*A*) Correlation between *MS4A4A* transcript expression and *FCGR3A* (*Left* panel) or *FCER1G* (*Right* panel). *P*-value and r coefficient were calculated according to the Spearman correlation test. (*B*) Multiple IF staining showing the colocalization between MS4A4A (yellow) and FCGR3A (in red, *Upper* panels) or FCER1G (in red, lower panel). $CD68^+$ macrophages are shown in green. White arrows on the merged images indicate triple-stained cells. Representative images are shown. (Scale bar, 50 μm.) (*C*) *FCGR3A* transcript expression in synovial tissues presenting a pauci-immune fibroid (F), diffuse-myeloid (M), or lympho-myeloid (L) pathotype, assessed by RNA-sequencing. *P*-values were calculated using the Kruskal–Wallis test with Dunn's posttest, $^{**}P < 0.01$, $^{***}P < 0.001$. (*D*) Correlation of *FCGR3A* transcript expression assessed by RNA-sequencing with the disease activity score/28 (DAS28, *Left* panel) and the (ESR, *Right* panel). *P*-value and r coefficient were calculated using the Pearson correlation test. (*E*) *Fcgr3a* transcript expression in BMDM from WT and KO mice treated or not with 1 μM of dexamethasone (Dex). *P*-values were calculated using the Mann–Whitney test, $^{**}P < 0.01$. (*F*) Synovial tissues of patients who did or did not receive corticosteroid (CS) treatment were stained for FCGR3A by IHC. Representative images are shown. (Scale bar, 50 μm.) (*G*) Percentage of $FCGR3A^+$ cells quantified by digital image analysis in the synovium of RA patients treated or not with CS. *P*-values were calculated using the Mann–Whitney test, $^{***}P < 0.001$. (*H*) Correlation between the percentage of $MS4A4A^+$ and the percentage of $FCGR3A^+$ synovial cells. *P*-value and r coefficient were calculated using the Pearson correlation test. (*I*) TNF and CXCL2 secretion by BMDM isolated from WT and KO mice and stimulated for 8 h with 500 μg/mL of IgG or 100 ng/mL lipopolysaccharides (LPS). 1 μM dexamethasone (Dex) was added on top IgG or LPS 1 h after the start of the stimulation. n = 4 to 10 per condition. (*J*) Tnf and *Cxcl2* transcript expression was assessed by RT-qPCR in the ankles of WT and KO mice treated with PBS or Dex at day 6 after STIA induction. n = 6 mice per group. *P*-values were calculated using the Kruskal–Wallis test with Dunn's posttest, $^{*}P < 0.05$, $^{**}P < 0{,}01$. (*C*, *E*, *G*, *I*, and *J*) Results are shown as mean ± SEM.

reduced neutrophil infiltration. The decreased neutrophil infiltrate correlated with lower expression of molecules involved in the regulation of matrix remodeling and bone erosions, leading to reduced cartilage and bone damage. Importantly, this effect was specific to CS, since *Ms4a4a* deletion had no influence on the therapeutic response to other immune-modulatory therapies, such as MTX or IVIg. Of note, while the STIA model is ideal to focus on the contribution of innate immune cells selectively to the effector phase of arthritis (30), and provides valuable insights into the understanding of the functional role of *Ms4a4a*, the differences between human and mouse pathophysiology, specifically the differences in neutrophil localization, emphasize the need for complementary studies to validate our findings.

The mechanism(s) responsible for the increased efficacy of CS in the absence of MS4A4A remains to be fully defined. We observed that Dex treatment was associated with reduced production of Tnf and the neutrophil-attracting chemokine Cxcl2 in macrophages lacking *Ms4a4a*, both in vitro and in the arthritis model in vivo, where this correlated with reduced synovial inflammation and number of recruited neutrophils. CS selectively induced the expression of FcγR3, both in vitro and in the RA synovium, and in vitro Dex-dependent reduction of Tnf and Cxcl2 in *Ms4a4a*-deficient macrophages was further enhanced by FcγR activation through aggregated IgG. Our results suggest that, by inducing the expression of MS4A4A and FcγR3, CS may amplify the response to immune complexes, which in turn would counteract their anti-inflammatory activity. MS4A4A is a tetraspan-like molecule (23, 24). Tetraspanins are membrane-organizing proteins clustering in tetraspanin-enriched microdomains (TEM). TEM are specific regions of the plasma membrane rich in lipids where tetraspanins can engage latero-lateral interactions with partner receptors and modulate their signaling pathways (23). Our previous work showed that in macrophages MS4A4A clusters with other members of the MS4A family, namely MS4A6A and MS4A7, and that it interacts with its receptor partners (e.g., Dectin-1) in the lipid rafts (24). Studies from us and others suggest that similar to tetraspanins, MS4A4A is a tuner of macrophage activation by modulating the activity of other surface receptors rather than by directly inducing an intracellular signal cascade (23). This supports the hypothesis that MS4A4A may regulate immunoglobulin-dependent signaling pathways by interacting with Fc receptors. Irrespective of the underlying mechanisms, the results reported here raise the interesting possibility that the upregulation of MS4A4A by CS may contribute to the development of tachyphylaxis/resistance while reciprocally the therapeutic inhibition of MS4A4A may allow lowering CS dosage and reduce their toxicity as well as address the issue of resistance to treatment, two key limiting factors in the therapeutic usage of CS in inflammatory diseases (46).

Overall, this study provides strong evidence that macrophage expression of MS4A4A is a correlate of synovial inflammation and disease severity in RA. In addition, as the MS4A4A upregulation by CS in vitro and in vivo limits their anti-inflammatory activity, macrophage MS4A4A may represent a biomarker of joint inflammation and a therapeutic target to amplify the action of CS.

Materials and Methods

Ethical Approvals. Studies including RA patients complied with the provisions of the Declaration of Helsinki and were approved by the National Research Ethics Service Committee London Dulwich (Rec number 05/Q0703/198 and 10/H0801/47). All patients were enrolled after giving their written informed consent. Procedures involving animals and their care were conformed with protocols approved by Humanitas Research Hospital (Milan, Italy) in compliance with national (D.L. N.116, G.U., suppl. 40, 18-2-1992 and N. 26, G.U. March 4, 2014) and international law and policies (EEC Council Directive 2010/63/ EU, OJ L 276/33, 22-09-2010; NIH Guide for the Care and Use of Laboratory Animals, US National Research Council, 2011). The study was approved by the Italian Ministry of Health (approvals n. 441/2019-PR, issued on 12/06/2019). All efforts were made to minimize the number of animals used and their suffering.

Patients. RA synovium samples were retrieved from either early (< 12 mo of symptoms) treatment-naïve RA patients recruited into the Pathobiology of Early Arthritis Cohort (http://www.peac-mrc.mds.qmul.ac.uk/; described as early RA) or from patients who had previously been treated with csDMARDs and/or with CS before commencing a biological therapy according to the UK NIH and Care Excellence prescribing guidelines (described as established RA). All patients fulfilled the American College of Rheumatology/European League Against Rheumatism 2010 RA classification criteria (47) and were enrolled at Bart's Health NHS Trust in London. Patients underwent an ultrasound-guided needle synovial biopsy (48), and synovial tissue samples were immediately fixed in 4% formaldehyde (Merck) and subsequently embedded in paraffin for histological characterization or preserved in RNA later (Ambion) for gene expression analysis. Clinical data, including the number of swollen and tender joints, patient VAS for pain, fatigue, global health, and physician assessment of global health were recorded, systemic levels of ESR and CRP were evaluated and DAS28 calculated for each patient. Structural damages were assessed at baseline and at 12 mo follow-up by scoring of hands and feet radiographs according to the SHSS by a single reader blinded to all clinical/histological data, as described previously (28). Clinical characteristics of the early and established RA cohorts are reported in *SI Appendix*, Tables S1 and S2.

Animal Colonies. Wild-type (WT) C57BL/6 J mice were obtained from Charles River Laboratories. Mice with a ubiquitous *Ms4a4a* inactivation (*Ms4a4a*-KO) were obtained by breeding mice carrying floxed *Ms4a4a* alleles ($Ms4a4a^{fl/fl}$) with mice expressing *Cre* under the control of the *ubiquitin* gene promoter ($B6.CgTg^{(UBC-Cre/ERT2)1Ejb/2}J$; Jackson Laboratory). *Ms4a4a*-KO mice were then backcrossed with C57BL/6 J mice to establish a colony generating *Ms4a4a*-KO and WT littermates. Animals with macrophage-specific *Ms4a4a* inactivation (*Ms4a4a*-cKO) were obtained as previously described (24). KO mice were cohoused with WT littermates in individually ventilated cages in a specific-pathogen-free animal facility.

Experimental Model of Arthritis. Experimental arthritis was induced as previously described (49), and the procedures are further described in *SI Appendix*.

Primary Cell Isolation and Stimulation. Murine BMDM from WT and KO mice were obtained as previously described (24, 50), and stimulated with 150 μg/mL IVIg (PrIVIgen), 500 μg/mL aggregated IgG prepared by stirring a 5 mg/mL IVIg solution in sodium citrate buffer (10 mM sodium citrate, 5% sucrose, pH 6.0) at room temperature (RT) for 20 h (51), or 100 ng/mL LPS (Sigma-Aldrich) for 6 h, then treated with 1 μM Dex for 8 or 18 h. Arthritic paws were collected, and pannus digested with Collagenase D and DNAse I (both from Roche) in Dulbecco's Modified Eagle's medium (Lonza). Cell suspensions were used to isolate joint macrophages (sMac) with the anti-F4/80 microbeads kit (Miltenyi Biotech) or fibroblast-like synoviocytes (FLS) by adhesion (52, 53). FLS were used between passages 3 and 8. Murine peritoneal macrophages (pMac) were elicited using 3% thioglycollate medium (Thermo Fisher Scientific) as previously described (54). sMac, pMac, and FLS were stimulated with 1 μM Dex for 18 h.

RNA Extraction and RNA Sequencing (RNA-Seq). RNA was extracted from total homogenized human synovial tissue and mouse joints or from primary cells using a Trizol/chloroform method or using the Direct-zol RNA-MiniPrep kit (Zymo Research). Bulk RNA-seq was performed on human synovium samples using an Illumina HiSeq2500 platform (Illumina), and raw data quality control, normalization, and analysis were performed as previously described (6). RNA obtained from mouse joints or primary cells was retrotranscribed using Superscript IV First-Strand Synthesis System (Thermo Fisher Scientific) or High-Capacity cDNA Reverse Transcription Kit (Applied Biosystems). Gene expression was quantified using TaqMan probes and primers, following the procedure described in *SI Appendix*.

Histology, IHC, and IF Staining. 3-μm-thick sections of formaldehyde-fixed human synovial tissue were prepared and stained with hematoxylin and eosin (H&E), and IHC was performed to define pathotypes, as previously described (5, 29, 55) and detailed in *SI Appendix*. In addition, synovial tissues were stained

for MS4A4A (Sigma-Aldrich), neutrophil elastase (NE; Novus Biologicals), and FCGR3A (Sigma-Aldrich). Formaldehyde-fixed mouse joints were decalcified (PFM Medical) prior to embedding, and sections were stained using H&E and TRAP protocols. Semiquantitative scores for H&E and TRAP were attributed on each section according to previously described methods (56, 57). Mouse Ly6G$^+$ neutrophils and Iba1$^+$ macrophages (both antibodies from Abcam) were stained by IHC. All slides were counterstained with hematoxylin and mounted with Distyrene Plasticizer Xylene mounting medium (Sigma-Aldrich). The percentage of MS4A4A, NE, FCGR3A, Ly6G, and Iba1-positive cells in the synovium was determined using quantitative digital image analyses (QuPath software) (58). All sections were digitally scanned using the Nanozoomer S210 in bright field (Hamamatsu Photonics). Multiple IF staining protocols are described in *SI Appendix*.

Flow Cytometry. Flow cytometry was performed on cell suspension obtained from mouse joint after tissue digestion (as described above), blood and bone marrow, and all related protocols are described in *SI Appendix*.

Enzyme-Linked Immunosorbent Assay. Cxcl2 and Tnf expression levels were measured in BMDM supernatants using the Ella automated immunoassay system (R&D Systems) as per the manufacturer's instructions.

Statistics. Statistical methods are described in *SI Appendix*.

Data, Materials, and Software Availability. The dataset generated in this study has been deposited in Zenodo (accession no. 14936162) (59). Additional study data are available as follows: raw RNA-seq data are deposited in the Gene Expression Omnibus (GEO) under accession number GSE302355 (https://www.ncbi.nlm.nih.gov/geo/query/acc.cgi?acc=GSE302355) (60). Previously published data were also used in this work; expression data were obtained from the ArrayExpress database (accession code E-MTAB-6141, https://www.ebi.ac.uk/biostudies/arrayexpress/studies/E-MTAB-6141) (61) and are referenced in previous publications 5, 6. All other data supporting the findings of this study are included in the manuscript and/or *SI Appendix*.

ACKNOWLEDGMENTS. This work was supported by departmental funds (Queen Mary University of London, Centre for Experimental Medicine and Rheumatology; Department of Inflammation and Immunology, Humanitas Clinical and Research Center; and Department of Medical Biotechnologies and Translational Medicine, University of Milan) as well as the Versus Arthritis Experimental Treatment Centre (infrastructure support; Grant 20022 to C.P.); the Medical Research Council (development of the Pathobiology of Early Arthritis Cohort cohort; Grant 36661 to C.P.); Fondazione Beppe e Nuccy Angiolini (to A.M.); the Italian Association for Cancer Research (Associazione Italiana per la Ricerca sul Cancro – Investigator (AIRC)–Special program: Metastatic disease: the key unmet need in oncology, Grant 21147, and AIRC-IG, Grant 30672 to A.M.); the Italian Ministry of University and Research (Grant Progetti di Ricerca di Interesse Nazionale (PRIN) 2017.0004386.29-03-2018 to M.L.); the Italian Ministry of University and Research (project "SCALE UP–Department of Excellence 2023-2027" to M.L.); PRIN 2022, "Finanziato dall'Unione europea–Next Generation EU Missione 4 Componente 1 Codice Unico di Progetto G53D23000720001" to E.M.B.; Fondation pour la recherche médicale (Grant ARF202004011786 to M.-A.B.); INSERM Aide à la Transition pour l'Installation de Projet-Avenir program (to M.-A.B.); Versus Arthritis Clinical Lectureship in Experimental Medicine and Rheumatology (Grant 21890 to A.N.); National Institute for Health and Care Research Transitional Research Fellowship (Grant TRF-2018-11-ST2-002) to F.R.; and Fundação para a Ciência e a Tecnologia; PhD Grant PD/BD/114138/2016 to R.S.-G. M.-A.B. is a recipient from the European Federation of Immunological Societies and Immunology Letters award short-term fellowship, European Molecular Biology Organization short-term fellowship, and European League Against Rheumatism scientific training grant for young fellows. I.M. is a recipient from European Federation of Immunological Societies and Immunology Letters award short-term fellowship and an AIRC Fellowship for Abroad. We thank all patients who participated to this study, the clinical staff who helped with recruitment, and the laboratory staff who helped with the processing of the histological samples. We thank Julie Foster and Katie Dexter for the guidance in Micro-computed tomography acquisition and analysis. We thank Silvano Sozzani, Annalisa Del Prete, and Francesca Sozio (Humanitas University), as well as Mauro Perretti and Dianne Cooper (Queen Mary University of London), for their assistance in providing arthritogenic serum and K/BxN transgenic mice.

Author affiliations: [a]Centre for Experimental Medicine & Rheumatology, William Harvey Research Institute and Barts and The London School of Medicine and Dentistry, Queen Mary University of London, London EC1M 6BQ, United Kingdom; [b]Nantes Université, Oniris, INSERM, Regenerative Medicine and Skeleton, Unité Mixte de Recherche 1229, Nantes F-44000, France; [c]Institute of Microbiology, Infectious Diseases and Immunology (I-MIDI), Charité-Universitätsmedizin Berlin Campus Benjamin Franklin, Berlin 12203, Germany; [d]Berlin Institute of Health, Berlin 12203, Germany; [e]Cellular and Humoral Innate Immunity Lab, Istituto di Ricovero e Cura a Carattere Scientifico Humanitas Research Hospital, Rozzano 20089, Milan, Italy; [f]Life and Health Sciences Research Institute, School of Medicine, University of Minho, Braga 4710-057, Portugal; [g]Life and Health Sciences Research Institute/Biomaterials, Biodegradables and Biomimetics Government Associate Laboratory, Braga/Guimarães 4710-057, Portugal; [h]Department of Medical Biotechnologies and Translational Medicine, University of Milan, Milan 20133, Italy; [i]Department of Anesthesiology, Critical Care, and Pain Medicine, Cardiac Anesthesia Division, Boston Children's Hospital, Boston, MA, 02115; [j]Clinical Proteomics Laboratory, Institute for Biomedical Technologies, Segrate 20054, Milan, Italy; [k]Institute for Genetic and Biomedical Research, Milan Unit, National Research Council, Milan 20090, Italy; and [l]Department of Biomedical Sciences, Humanitas University, Pieve Emanuele 20972, Milan, Italy

Author contributions: M.-A.B., I.M., R.S.-G., B.B., M.L., A.M., and C.P. designed research; M.-A.B., I.M., R.S.-G., A.N., M.S., G.M.G., A.T., S.G., F.R., E.M.B., and C.S. performed research; M.-A.B., I.M., R.S.-G., C.C., K.G., A.R.P., D.D.S., A.L., E.M.B., and M.J.L. analyzed data; M.-A.B. initiated the project, developed the animal models of arthritis, and led the human part of the study; I.M. brought expertise of MS4A molecules and flow cytometry analysis, and contributed to overall study design; R.S.-G. analyzed in vivo data and completed in vitro experiments; M.-A.B., A.N., and G.M.G. performed histology, immunohistochemistry and immunofluorescence staining and analysis; M.-A.B., I.M., R.S.-G., and M.S. performed in vitro and in vivo experiments and associated analysis; F.R., M.J.L., and C.P. recruited patients and helped access patient samples; C.C., K.G., A.R.P., D.D.S., A.L., and M.J.L. performed RNA-sequencing analysis; and M.-A.B., I.M., R.S.-G., B.B., M.L., A.M., and C.P. wrote the paper.

1. S. Safiri *et al.*, Global, regional and national burden of rheumatoid arthritis 1990–2017: A systematic analysis of the Global Burden of Disease study 2017. *Ann. Rheum. Dis.* **78**, 1463–1471 (2019).
2. D. Aletaha, J. S. Smolen, Diagnosis and management of rheumatoid arthritis: A review. *JAMA* **320**, 1360 (2018).
3. M. Doumen, S. Pazmino, D. Bertrand, R. Westhovens, P. Verschueren, Glucocorticoids in rheumatoid arthritis: Balancing benefits and harm by leveraging the therapeutic window of opportunity. *Joint Bone Spine* **90**, 105491 (2023).
4. L. T. Donlin *et al.*, Insights into rheumatic diseases from next-generation sequencing. *Nat. Rev. Rheumatol.* **15**, 327–339 (2019).
5. F. Humby *et al.*, Synovial cellular and molecular signatures stratify clinical response to csDMARD therapy and predict radiographic progression in early rheumatoid arthritis patients. *Ann. Rheum. Dis.* **78**, 761–772 (2019).
6. M. J. Lewis *et al.*, Molecular portraits of early rheumatoid arthritis identify clinical and treatment response phenotypes. *Cell Rep.* **28**, 2455–2470.e5 (2019).
7. G. Lliso-Ribera *et al.*, Synovial tissue signatures enhance clinical classification and prognostic/treatment response algorithms in early inflammatory arthritis and predict requirement for subsequent biological therapy: Results from the pathobiology of early arthritis cohort (PEAC). *Ann. Rheum. Dis.* **78**, 1642–1652 (2019).
8. A. Nerviani *et al.*, A pauci-immune synovial pathotype predicts inadequate response to TNFα-blockade in rheumatoid arthritis patients. *Front. Immunol.* **11**, 845 (2020).
9. J. J. Haringman *et al.*, Synovial tissue macrophages: A sensitive biomarker for response to treatment in patients with rheumatoid arthritis. *Ann. Rheum. Dis.* **64**, 834–838 (2005).
10. G. Dennis *et al.*, Synovial phenotypes in rheumatoid arthritis correlate with response to biologic therapeutics. *Arthritis Res. Ther.* **16**, R90 (2014).
11. D. E. Orange *et al.*, Identification of three rheumatoid arthritis disease subtypes by machine learning integration of synovial histologic features and RNA sequencing data. *Arthritis Rheumatol.* **70**, 690–701 (2018).
12. F. Rivellese *et al.*, Rituximab versus tocilizumab in rheumatoid arthritis: Synovial biopsy-based biomarker analysis of the phase 4 R4RA randomized trial. *Nat. Med.* **28**, 1256–1268. (2022), 10.1038/s41591-022-01789-0.
13. F. Humby *et al.*, Rituximab versus tocilizumab in anti-TNF inadequate responder patients with rheumatoid arthritis (R4RA): 16-week outcomes of a stratified, biopsy-driven, multicentre, open-label, phase 4 randomised controlled trial. *Lancet* **397**, 305–317 (2021).
14. A. Di Matteo, J. M. Bathon, P. Emery, Rheumatoid arthritis. *Lancet* **402**, 2019–2033 (2023).
15. Fan Zhang *et al.*, Defining inflammatory cell states in rheumatoid arthritis joint synovial tissues by integrating single-cell transcriptomics and mass cytometry. *Nat. Immunol.* **20**, 928–942 (2019).
16. M.-A. Boutet *et al.*, Novel insights into macrophage diversity in rheumatoid arthritis synovium. *Autoimmun. Rev.* **20**, 102758 (2021).
17. P. J. Murray, Macrophage polarization. *Annu. Rev. Physiol.* **79**, 541–566 (2017).
18. M. Locati, G. Curtale, A. Mantovani, Diversity, mechanisms, and significance of macrophage plasticity. *Annu. Rev. Pathol.* **15**, 123–147 (2020).
19. M. D. Park, A. Silvin, F. Ginhoux, M. Merad, Macrophages in health and disease. *Cell* **185**, 4259–4279 (2022).
20. S. Alivernini *et al.*, Distinct synovial tissue macrophage subsets regulate inflammation and remission in rheumatoid arthritis. *Nat. Med.* **26**, 1295–1306 (2020).

21. K. Ishibashi, M. Suzuki, S. Sasaki, M. Imai, Identification of a new multigene four-transmembrane family (MS4A) related to CD20, HTm4 and beta subunit of the high-affinity IgE receptor. *Gene* **264**, 87–93 (2001).
22. R. Silva-Gomes *et al.*, Differential expression and regulation of MS4A family members in myeloid cells in physiological and pathological conditions. *J. Leukoc. Biol.* **111**, 817–836 (2022).
23. I. Mattiola, A. Mantovani, M. Locati, The tetraspan MS4A family in homeostasis, immunity, and disease. *Trends Immunol.* **42**, 764–781 (2021).
24. I. Mattiola *et al.*, The macrophage tetraspan MS4A4A enhances dectin-1-dependent NK cell–mediated resistance to metastasis. *Nat. Immunol.* **20**, 1012–1022 (2019).
25. Y. Deming *et al.*, The MS4A gene cluster is a key modulator of soluble TREM2 and Alzheimer's disease risk. *Sci. Transl. Med.* **11**, eaau2291 (2019).
26. M. Colonna, The biology of TREM receptors. *Nat. Rev. Immunol.* **23**, 580–594 (2023).
27. E. Corsiero, A. Nerviani, M. Bombardieri, C. Pitzalis, Ectopic lymphoid structures: Powerhouse of autoimmunity. *Front. Immunol.* **7** (2016).
28. F. Humby *et al.*, Synovial cellular and molecular signatures stratify clinical response to csDMARD therapy and predict radiographic progression in early rheumatoid arthritis patients. *Ann. Rheum. Dis.* **78**, 761–772 (2019). https://doi.org/10.1136/annrheumdis-2018-214539.
29. C. Pitzalis, S. Kelly, F. Humby, New learnings on the pathophysiology of RA from synovial biopsies. *Curr. Opin. Rheumatol.* **25**, 334–344 (2013).
30. A. D. Christensen, C. Haase, A. D. Cook, J. A. Hamilton, K/BxN serum-transfer arthritis as a model for human inflammatory arthritis. *Front. Immunol.* **7**, 213 (2016).
31. C. M. Termini, J. M. Gillette, Tetraspanins function as regulators of cellular signaling. *Front. Cell Dev. Biol.* **5**, 34 (2017).
32. Y. Zuo, G.-M. Deng, Fc gamma receptors as regulators of bone destruction in inflammatory arthritis. *Front. Immunol.* **12**, 688201 (2021).
33. S. E. Magnusson, E. Wennerberg, P. Matt, U. Lindqvist, S. Kleinau, Dysregulated Fc receptor function in active rheumatoid arthritis. *Immunol. Lett.* **162**, 200–206 (2014).
34. M. A. Murayama, J. Shimizu, C. Miyabe, K. Yudo, Y. Miyabe, Chemokines and chemokine receptors as promising targets in rheumatoid arthritis. *Front. Immunol.* **14**, 1100869 (2023).
35. G. Pavlasova, M. Mraz, The regulation and function of CD20: An "enigma" of B-cell biology and targeted therapy. *Haematologica* **105**, 1494–1506 (2020).
36. M. D. Cohen, E. Keystone, Rituximab for rheumatoid arthritis. *Rheumatol. Ther.* **2**, 99–111 (2015).
37. H. M. Gürcan *et al.*, A review of the current use of rituximab in autoimmune diseases. *Int. Immunopharmacol.* **9**, 10–25 (2009).
38. D. Supino *et al.*, Monocyte–macrophage membrane expression of IL-1R2 is a severity biomarker in sepsis. *Cell Death Dis.* **16**, 269 (2025).
39. A. A. Seyhan *et al.*, Novel biomarkers of a peripheral blood interferon signature associated with drug-naïve early arthritis patients distinguish persistent from self-limiting disease course. *Sci. Rep.* **10**, 8830 (2020).
40. A. Wierczeiko *et al.*, A call for gene expression analysis in whole blood of patients with rheumatoid arthritis (RA) as a biomarker for RA-associated interstitial lung disease. *J. Rheumatol.* **51**, 130–133 (2024).
41. A. Mantovani, C. Garlanda, Humoral innate immunity and acute-phase proteins. *N. Engl. J. Med.* **388**, 439–452 (2023).
42. M. Perretti, F. D'Acquisto, Annexin A1 and glucocorticoids as effectors of the resolution of inflammation. *Nat. Rev. Immunol.* **9**, 62–70 (2009).
43. J. M. Ehrchen, J. Roth, K. Barczyk-Kahlert, More than suppression: Glucocorticoid action on monocytes and macrophages. *Front. Immunol.* **10**, 2028 (2019).
44. A. W. Jubb, S. Boyle, D. A. Hume, W. A. Bickmore, Glucocorticoid receptor binding induces rapid and prolonged large-scale chromatin decompaction at multiple target loci. *Cell Rep.* **21**, 3022–3031 (2017).
45. J.-P. Auger *et al.*, Metabolic rewiring promotes anti-inflammatory effects of glucocorticoids. *Nature* **629**, 184–192 (2024).
46. P. J. Barnes, I. M. Adcock, Glucocorticoid resistance in inflammatory diseases. *Lancet* **373**, 1905–1917 (2009).
47. D. Aletaha *et al.*, 2010 rheumatoid arthritis classification criteria: An American College of Rheumatology/European League Against Rheumatism collaborative initiative. *Ann. Rheum. Dis.* **69**, 1580–1588 (2010).
48. S. Kelly *et al.*, Ultrasound-guided synovial biopsy: A safe, well-tolerated and reliable technique for obtaining high-quality synovial tissue from both large and small joints in early arthritis patients. *Ann. Rheum. Dis.* **74**, 611–617 (2015).
49. P. A. Monach, D. Mathis, C. Benoist, The K/BxN arthritis model. *Curr. Protoc. Immunol.* **15**, 15.22.1–15.22.12 (2008).
50. L. Carretero-Iglesia, M. Hill, M. C. Cuturi, Generation and characterization of mouse regulatory macrophages. *Methods Mol. Biol.* **1371**, 89–100 (2016).
51. S. K. Polumuri, L. A. Haile, D. D. C. Ireland, D. Verthelyi, Aggregates of IVIG or Avastin, but not HSA, modify the response to model innate immune response modulating impurities. *Sci. Rep.* **8**, 11477 (2018).
52. M.-A. Boutet *et al.*, Distinct expression of interleukin (IL)-36α, β and γ, their antagonist IL-36Ra and IL-38 in psoriasis, rheumatoid arthritis and Crohn's disease. *Clin. Exp. Immunol.* **184**, 159–173 (2016).
53. M.-A. Boutet *et al.*, Interleukin-36 family dysregulation drives joint inflammation and therapy response in psoriatic arthritis. *Rheumatology* **59**, 828–838 (2020).
54. X. Zhang, R. Goncalves, D. M. Mosser, The isolation and characterization of murine macrophages. *Curr. Protoc. Immunol.* **14**, 14.1.1–14.1.14 (2008).
55. V. Krenn *et al.*, Synovitis score: Discrimination between chronic low-grade and high-grade synovitis. *Histopathology* **49**, 358–364 (2006).
56. W. O'Brien *et al.*, RANK-independent osteoclast formation and bone erosion in inflammatory arthritis: Osteoclast formation in inflamed joints. *Arthritis Rheumatol.* **68**, 2889–2900 (2016).
57. M.-A. Boutet *et al.*, IL-38 overexpression induces anti-inflammatory effects in mice arthritis models and in human macrophages in vitro. *Ann. Rheum. Dis.* **76**, 1304–1312 (2017).
58. P. Bankhead *et al.*, QuPath: Open source software for digital pathology image analysis. *Sci. Rep.* **7**, 16878 (2017).
59. M.-A. Boutet *et al.*, Dataset related to article "Synovial MS4A4A correlates with inflammation and counteracts response to corticosteroids in arthritis." Zenodo. https://zenodo.org/uploads/14936162. Deposited 27 February 2025.
60. A. Putignano *et al.*, Synovial MS4A4A correlates with inflammation and counteracts response to corticosteroids in arthritis. Gene Expression Omnibus (GEO). https://www.ncbi.nlm.nih.gov/geo/query/acc.cgi?acc=GSE302355. Deposited 11 July 2025.
61. C. John, M. Lewis, Comprehensive transcriptome analysis of synovium and peripheral *blood* reveals major disease heterogeneity early in the RA disease process prior to therapeutic intervention. BioStudies. https://www.ebi.ac.uk/biostudies/arrayexpress/studies/E-MTAB-6141. Accessed October 2020.